Biomimetic Hydrolysis of Penicillin G Catalyzed by Dinuclear Zinc(II) Complexes: Structure–Activity Correlations in β-Lactamase Model Systems

Bernhard Bauer-Siebenlist, Sebastian Dechert, and Franc Meyer*[a]

Abstract: A series of highly preorganized pyrazolate-based dinuclear zinc complexes has been studied as functional synthetic analogues of metallo-β-lactamases, a class of bacterial enzymes that cause serious clinical problems because of their degradation of common β-lactam antibiotics. We have investigated the hydrolytic cleavage of penicillin G mediated by the different dinuclear zinc complexes, and have deduced structure–activity correlations. While cooperative effects of the adjacent metal ions might be operative, these are found to either enhance or diminish β-lactamase activity with respect to a single free zinc. Drastic differences in activity are ascribed to a lack of accessible binding sites after incorporation of the substrate within the bimetallic pocket of **2** and **4**, whereas partial detachment of hemilabile ligand side arms in **1** and **3** opens up available coordination sites for nucleophile activation and/or for binding and polarisation of the β-lactam amide oxygen atom. This interpretation has been corroborated by NMR spectroscopic and mass spectrometric evidence as well as by X-ray crystallography of several adducts formed between the pyrazolate-based dinuclear zinc scaffolds and the small substrate analogue oxazetidinylacetate (oaa), **5**–**7**. In all adducts, the carboxylate group of oaa is the primary anchoring site and is nested in a bridging position within the bimetallic pocket. However, zinc binding of the β-lactam amide oxygen atom has been confirmed crystallographically for the first time in **7**, in which additional open-site coordination sites are available.

Keywords: antibiotics · bioinorganic chemistry · lactams · metallohydrolase models · zinc

Introduction

β-Lactamases are a class of enzymes that efficiently catalyze the hydrolytic opening of β-lactam rings.[1,2] Since the β-lactam motif is a crucial subunit of the largest group of therapeutically useful antibiotics, comprising the penicillin, cephalosporin, and carbapenem families, bacteria express β-lactamases in order to escape the action of these important β-lactam antibiotics. Nowadays, increasing resistance against β-lactam antibiotics poses a serious clinical problem.[3–5]

Known β-lactamase enzymes are usually grouped into several classes.[6] Most abundant are the various serine β-lactamases, the catalytic mechanism of which involves an acyl intermediate formed by nucleophilic attack of an active-site serine residue on the β-lactam.[2,7,8] Over the years, successful inhibitors such as sulbactam have been developed for this class of β-lactamases. Unfortunately, serine β-lactamase inhibitors are inactive towards enzymes of the other class of β-lactamases, which depend on one or two zinc(II) ions within their active site.[9–11] These so-called metallo-β-lactamases are less common, but hydrolyze a wide range of substrates. Since clinically useful inhibitors are not yet available, their spread to pathogenic species has raised the concern of the biomedical community.[3,5,9] A detailed mechanistic picture of metallo-β-lactamase action is not only of fundamental interest, but may also contribute to the development of efficient mechanism-based inhibitors.

Sequence information and X-ray crystal structures are known for several metallo-β-lactamases, in particular for the enzymes from *Bacillus cereus* and *Bacteroides fragilis*.[11,12] The majority of these have similar asymmetric dinuclear zinc-binding motifs with three histidine residues bound to the first zinc ion and a cysteine thiolate, the carboxylate group of an aspartate, another histidine residue, and a water molecule bound to the second zinc atom (Figure 1).[13–18] Either a typical tightly bridged form **A** or a so-called loosely bridged form with larger Zn···Zn separation have been detected in some of the crystallographic work on proteins

[a] Dr. B. Bauer-Siebenlist, Dr. S. Dechert, Prof. Dr. F. Meyer
Institut für Anorganische Chemie
der Georg-August-Universität Göttingen
Tammannstrasse 4, 37077 Göttingen (Germany)
Fax: (+49) 551-393-063
E-mail: franc.meyer@chemie.uni-goettingen.de

Supporting information for this article is available on the WWW under http://www.chemeurj.org/ or from the author.

 DOI: 10.1002/chem.200401272

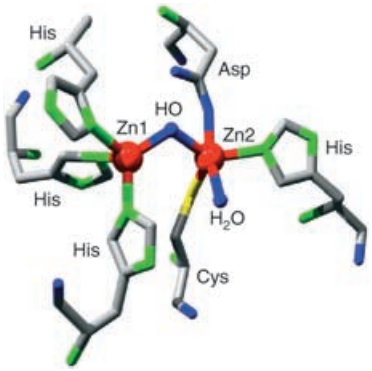

Figure 1. The active site structure of *B. fragilis* β-lactamase.[14]

from different organisms.[14,17] The latter has been reproduced by a shared water/hydroxide structure **B** in quantum

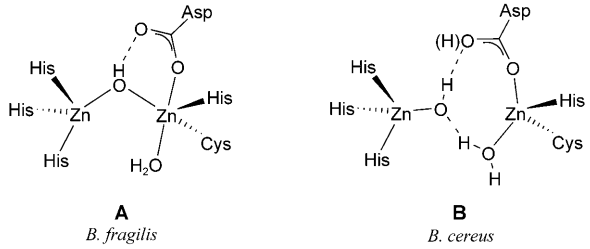

chemical studies and molecular dynamics (MD) simulations for the *B. fragilis* and *B. cereus* enzymes in their free and substrate-complexed forms,[19–21] and such a more flexible non-bridged form (**B**) may best be described as an O_2H_3 unit between the two zinc ions. The Zn···Zn separations are hence found to vary between 3.4 (**A**) and 4.4 Å (**B**).

Although the dinuclear zinc form of metallo-β-lactamases from *B. fragilis* and *B. cereus* is usually considered as the biologically active one, the role of the second Zn^{2+} ion remains controversial, since the affinity of the enzyme for the two metal ions may differ drastically (with comparable affinity for both zinc ions in the case of *B. fragilis*, but much lower affinity for the second zinc ion in *B. cereus*).[22,23] Furthermore, activity is also observed for the mononuclear species and distinct mechanisms may be relevant for the mono- and bimetallic forms.[12,23–25] Details of the catalysis by dinuclear zinc metallo-β-lactamases are still a subject of controversy, although it is generally postulated that interaction of the β-lactam carbonyl group with a zinc ion polarizes the C–O bond and allows nucleophilic attack by a metal-bound hydroxide with fission of the C–N bond. Subsequent protonation of the β-lactam nitrogen atom and dissociation of the acyl group would liberate the ring-opened product (Scheme 1).[24]

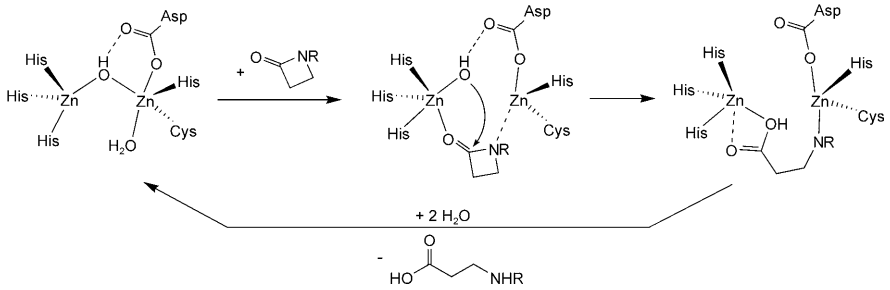

Scheme 1. Proposed mechanism of metallo-β-lactamase.

While the exact identity and position of the nucleophile is unclear, calculations led to the proposal that substrate binding may induce rupture of the hydroxide bridge and an increase in Zn···Zn separation in order to enhance nucleophilicity of the hydroxide group.[19–21] The pH profiles of the *B. cereus* reaction indicate that the second zinc(II) is not required for nucleophile activation, but it has been proposed that it may play a role in orienting the attacking nucleophile and in stabilizing reaction intermediates.[24,26–28] A ring-opened form of the substrate could be detected as an intermediate in the hydrolysis of nitrocefin by the *B. fragilis* enzyme,[29] and its identity as a zinc(II)-bound N-deprotonated species that results upon C–N bond-cleavage has been corroborated by model studies.[30]

While several groups have dealt with the hydrolysis or methanolysis of β-lactams by using simple transition-metal salts including Zn^{2+} salts,[31,32] very few studies have employed preorganized dinuclear zinc(II) complexes as functional mimics of metallo-β-lactamases.[30,33,34] Such models might provide valuable insights into the mechanistic role of the second Zn^{2+} ion, cooperative effects of the adjacent metal ions, and the identity of the active nucleophile. Lippard and co-workers recently reported an in-depth study of nitrocefin hydrolysis mediated by phenol- and naphtyridine-based dinuclear zinc complexes.[33,34] From the observation that some mononuclear zinc(II) complexes are as efficient in nitrocefin hydrolysis as the dinuclear zinc(II) complexes they concluded that the second Zn^{2+} is not required for catalytic activity. Depending on the specific system, either a bridging or a terminal hydroxide was found to act as the nucleophile.[33,34] Preferential metal-ion coordination of β-lactam substrates by means of a monodentate carboxylate group was inferred from ^{13}C NMR and IR spectroscopy.[33,34]

Here we report a comparative study on the hydrolytic cleavage of penicillin G (pen) mediated by the recently reported dinuclear zinc(II) complexes **1**–**4**,[35–37] as well as structural and spectroscopic insights into the mode of substrate binding. Complexes **1**–**4** are based on multifunctional pyrazolate ligands HL^1–HL^4, which offer the advantage to constrain the accessible range of metal–metal separation by

means of the lengths of the chelating side arms attached to the heterocycle.[36,38–40] Hence, a Zn···Zn separation >4 Å

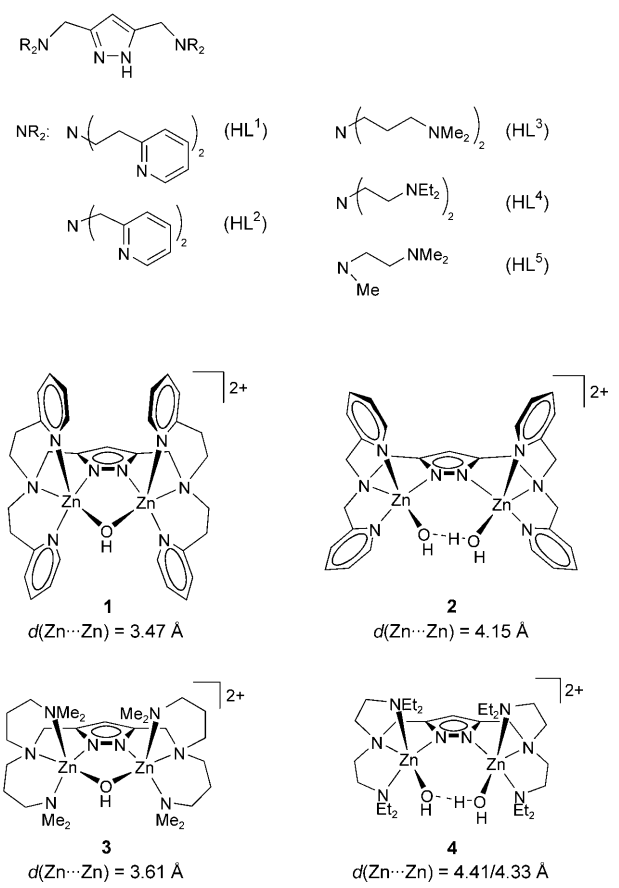

occurs in complexes **2** and **4** with shorter chelate arms, giving rise to a labile O_2H_3 unit within the bimetallic pocket, while **1** and **3** feature much shorter Zn···Zn separations of ~3.5 Å and a more tightly bound bridging hydroxide group.[35–37] Previous work on these complexes has indicated that the pK_a of Zn-bound water may be lowered even more drastically if the resulting hydroxide group is involved in strong intramolecular hydrogen bonding in the O_2H_3 moiety than if trapped in a bridging position between the two metal ions. The corresponding acids of **2** and **4** were found to have pK_a values of 7.60 and 7.57, respectively, while that of **1** has a pK_a value of 7.96 (dinuclear zinc complexes of HL^3 are not sufficiently stable in aqueous solution).[36–38,41]

It is interesting to note that the different situations of a Zn-O(H)-Zn bridge in **1**, **3** versus a Zn-O_2H_3-Zn bridge in **2**, **4** closely resemble the two active-site model configurations **A** ("tightly bridged") and **B** ("loose" or "nonbridged") described above, with Zn···Zn separations of ~3.5 and ~4.4 Å, respectively. The Zn-O_2H_3-Zn unit has previously been proposed as a structural and possibly functional motif in oligozinc enzymes,[35,42] and most recently this has been supported by DFT calculations on the bovine lens leucine aminopeptidase (*bl*LAP) active site.[43]

Since adducts of complexes **1**–**4** with penicillin G (or its hydrolytically cleaved form) could not be obtained as single crystals, for binding studies we also used simple β-lactams such as *N*-benzylazetidinone (nba) and oxazetidinylacetate (oaa), which contain essential structural elements of the common antibiotics (β-lactam amide or β-lactam amide and carboxylate, respectively). The β-lactams used in this work comprise penicillin G (pen), 2-oxazetidinylacetate (oaa), and cephalothin (ceph), and are shown below.

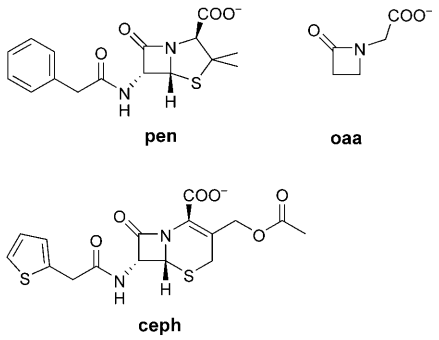

Results and Discussion

Hydrolysis of penicillin G by dinuclear zinc(II) complexes: We followed the time-course of penicillin G hydrolysis mediated by complexes **1**–**4** by in-situ FT-IR spectroscopy. IR spectra of β-lactams show a strong band for the lactam C=O valence vibration. Its position is markedly shifted towards higher wavenumbers relative to absorptions of carboxyesters, amides, and carboxylic acids, and the isolated position of the penicillin G lactam C=O stretch at 1768 cm^{-1} allows a quantitative evaluation (see Figure 2). The appearance of a new band for the carboxylate of the ring-opened product around 1650 cm^{-1} adds an independent measure.

When complexes **1**–**4** were added to solutions of penicillin G (four equivalents in DMSO/water 9:1)[44] and IR spectral changes were followed over several hours, gradual disappearance of the β-lactam ν(C=O) band could be observed in most cases. Control experiments with simple Zn^{2+} salts such as $Zn(NO_3)_2 \cdot 6H_2O$ or $Zn(ClO_4)_2 \cdot 6H_2O$ and experiments under basic conditions (KO*t*Bu) in the absence of zinc ions were carried out for comparison. This was expected to reveal the contribution from general base and single-site reactivity, and to provide additional information on the effect of preorganization of the dinuclear zinc center. Plots of the concentration ratio penicillin G/complex versus time are shown in Figure 3. No significant differences were observed for $Zn(NO_3)_2 \cdot 6H_2O$ and $Zn(ClO_4)_2 \cdot 6H_2O$, confirming that these salts are dissociated and that the anion has no influence.

Drastic differences in hydrolytic efficiency for the various systems are apparent. KO*t*Bu (without Zn^{2+}) and complex **4** are inactive and barely promote the cleavage of penicillin G within the time-frame investigated. For all other compounds the reaction rate increases in the order $\mathbf{2} < Zn^{2+} < \mathbf{1} < \mathbf{3}$, and

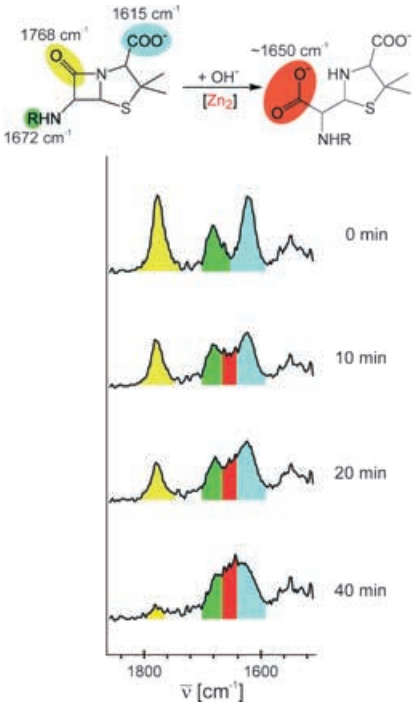

Figure 2. IR spectral changes during the hydrolysis of penicillin G mediated by **3** in DMSO/water (9:1).

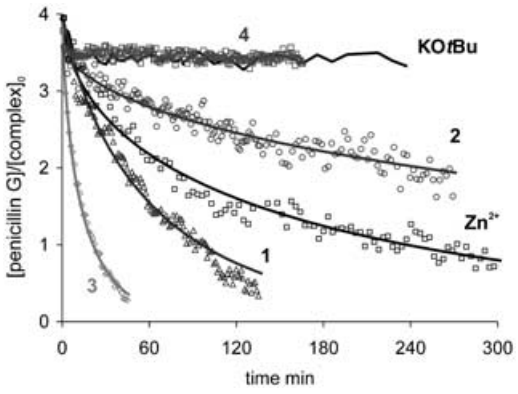

Figure 3. Time course of hydrolytic cleavage of four equivalents of penicillin G promoted by complex **1**, **2**, **3**, **4**, KO*t*Bu, or $Zn(ClO_4)_2 \cdot 6H_2O$ in DMSO/water 9:1 (v/v). In the case of **1**, **2**, **3**, and Zn^{2+}, the solid lines are meant as a guide to the eye.[45]

simple base hydrolysis can thus be ruled out. While the activity for **2** is less efficient than that for free zinc, **1** and **3** show significantly enhanced activity. In particular, in the presence of **3**, three out of four equivalents of penicillin G are cleaved within around 20 min. Cooperative effects of the adjacent metal ions might thus be operative (either enhancing or diminishing β-lactamase activity with respect to a single free zinc), but these effects apparently depend on the particular molecular arrangement that is determined by the ligand scaffold.

Characteristic Michaelis–Menten-type behavior involving a substrate-binding pre-equilibrium had been observed previously for phosphate diester hydrolysis mediated by pyrazolate-based dinuclear zinc complexes.[36,37] A similar mechanistic scheme is assumed here, but unfortunately the small concentration range available under the experimental setup hampered any comprehensive kinetic analysis.[45] To get some insight in the molecular causes for the trends in reactivity evident from Figure 3, substrate binding has been studied in more detail. It should be noted that cephalothin is not cleaved to any significant extent by any of the present complexes within several hours, in accordance with the known higher stability of cephalosporins over penicillins.

Binding of β-lactam substrates in solution: In β-lactam antibiotics such as penicillin G, several potential donor groups are available for metal-ion binding. These comprise the carboxylate, the β-lactam amide (through N or O atoms), the appended amide function, or the thioether (through the S atom). The mode of coordination depends on the metal and on the particular substrate and is usually inferred from spectroscopic data, while structural information is very scarce. Here, binding of penicillin G (and cephalothin) to complexes **1**–**4** has been investigated by means of electrospray ionization (ESI) mass spectrometry as well as IR and NMR spectroscopy; the simple substrate analogue oxazetidinylacetate (oaa) was used for crystallographic work.

Upon addition of the active complexes **1** or **3** to a solution of the substrate in DMSO/aqueous TRIS buffer (8:2) at pH 7.32, 7.83, or 8.47, a change of the β-lactam ν(C=O) absorption from 1768 to around 1749 cm^{-1} was observed within the first few minutes. The intensity of the latter band then decreased gradually due to hydrolytic cleavage of the lactam ring. A shift of 25–50 cm^{-1} for ν(C=O) to lower wavenumbers has been reported as indicative of metal-ion coordination to the β-lactam oxygen atom.[46] It should be noted, however, that prior to the onset of the hydrolytic reaction we observed no major spectral changes upon mixing of the complexes and penicillin G in a DMSO/water mixture in the absence of TRIS buffer. The cause for this effect of TRIS buffer (which is present in a large excess at concentrations of 0.1–1.0 M) is not clear at present, but it gives a further reason for the use of nonbuffered DMSO/water in the hydrolysis experiments described above.

The ^{13}C NMR spectra of the hydrolytically more inert cephalothin in the presence of complexes **1** or **2** in [D_6]DMSO reveal a noticable downfield shift of the carboxylate signal from 163.8 (free cephalothin) to 166.7 (**1**) or 165.8 ppm (**2**), but only a minor downfield shift for the lactamic ^{13}C NMR resonance from 162.8 to 164.1 (**1**) or 164.2 ppm (**2**). The positions of the carbonyl signals for the ester group and for the appended amide do not change significantly (less than 1 ppm). Since a downfield shift of the carbonyl ^{13}C NMR resonance is characteristic for metal-ion coordination, the NMR data clearly suggest that zinc binds to the carboxylate group, while the involvement of the β-lactam oxygen atom in zinc coordination remains ambiguous.

ESI mass spectra of solutions of complexes **1**–**4** in methanol[47] containing one equivalent of penicillin G or cephalo-

thin reveal dominant peaks for species $[Zn_2(L)(pen)(OMe)]^+$ or $[Zn_2(L)(ceph)(OMe)]^+$, respectively. In some cases, minor signals characteristic for $[Zn_2(L)(pen)_2(MeOH)_2]^+$ or $[Zn_2(L)(ceph)_2]^+$ are also detected. The spectrum for **1**/penicillin G is depicted in Figure 4 as an example.

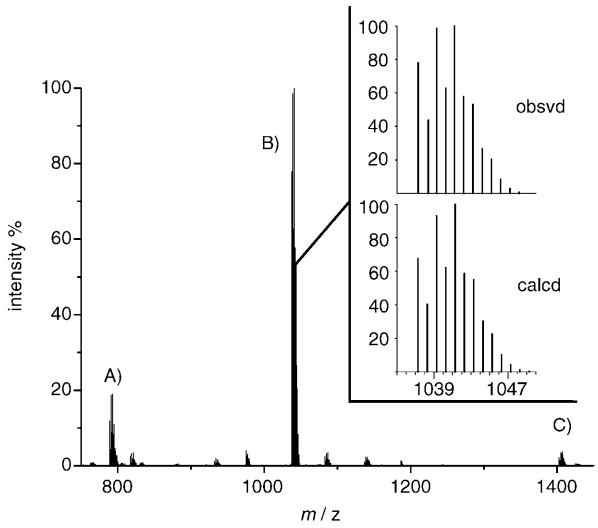

Figure 4. ESI MS spectra of **1**/penicillin G in MeOH; A) $[Zn_2(L^1)(OH)(ClO_4)]^+$; B) $[Zn_2(L^1)(pen)(OMe)]^+$; C) $[Zn_2(L^1)(pen)_2(MeOH)_2]^+$. The inset shows the experimental and calculated isotopic distribution for peak B.

IR spectroscopy proved informative for further characterization of the major $[Zn_2(L)(pen)(OMe)]^+$ species observed in the ESI mass spectra and to differentiate between possible substrate binding modes. After mixing the respective complex **1**–**4** with an equimolar amount of penicillin G in methanol/DMSO (1:1), the β-lactam ν(C=O) absorption changes significantly from 1773 to around 1740 cm^{-1}, while shifts are only minor (from 1616 to around 1610 cm^{-1}) for the carboxylate group. The ν(C=O) absorption at ~1740 cm^{-1} is in the range characteristic for carboxylic esters and may indicate that in the $[Zn_2(L)(pen)(OMe)]^+$ species detected by ESI mass spectrometry the β-lactam ring has been cleaved by methanol to give a methyl ester. On the other hand, the analogous $[Zn_2(L)(ceph)(OMe)]^+$ species could be observed by ESI-MS for mixtures of the complexes and cephalothin, despite that fact that the more inert cephalothin is not hydrolyzed by **1**–**4**. This suggests that in the $[Zn_2(L)(pen)(OMe)]^+$ and $[Zn_2(L)(ceph)(OMe)]^+$ species the β-lactam ring is still intact and a distinct Zn-bound methoxide is present besides the bound substrate. It should be noted that ESI mass spectra of solutions of complexes **1**–**4** and N-benzylazetidinone (nba) in methanol show prominent signals for the respective $[Zn_2(L)(OMe)(ClO_4)]^+$ ions, but there is no evidence for bound nba. Here the β-lactam derivative is at best loosely bound, in accordance with the carboxylate being the major anchoring site for pen and ceph, but again a Zn-bound methoxide is present.

To elucidate the binding mode of β-lactam derivatives that feature both the β-lactam C=O and a carboxylate group in the α-position to the lactam-N, the small substrate analogue oxacetidinylacetate (oaa) is more appropriate than nba.

Solid-state structures of adducts between dinuclear zinc complexes and oxazetidinylacetate: Since adducts between complexes **1**–**4** and antibiotics penicillin G or cephalosporin (or their cleavage products) could not be obtained in crystalline form, we turned to oxazetidinylacetate (oaa) as a substrate mimic that features the essential structural fragments of penicillin with both the β-lactam amide and the free carboxylate groups as potential metal-ion binding sites. Single crystals of complexes $[Zn_2(L^4)(oaa)](ClO_4)_2$ (**5**) and $[Zn_2(L^3)(oaa)_2](H_3O)(ClO_4)_2$ (**6**) were analyzed by X-ray crystallography, and molecular structures of the cations are shown in Figures 5 and 6.

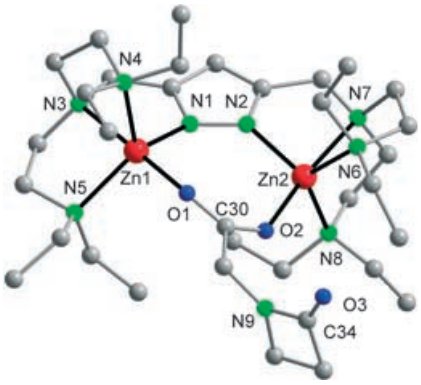

Figure 5. View of the molecular structure of complex **5**. In the interest of clarity, all protons have been omitted. Selected interatomic distances (Å) and angles (°): Zn1–O1 2.014(2), Zn1–N1 2.013(2), Zn1–N3 2.250(2), Zn1–N4 2.157(2), Zn1–N5 2.141(2), Zn2–O2 2.020(2), Zn2–N2 2.013(2), Zn2–N6 2.2802, Zn2–N7 2.162(2), Zn2–N8 2.146(2), Zn1···Zn2 4.1842(5), N1–N2 1.377(3), O1–C30 1.251(3), O2–C30 1.262(3), N9–C34 1.354(4), O3–C34 1.218(4), N1-Zn1-O1 101.17(8), N1-Zn1-N5 127.60(9), O1-Zn1-N5 96.95(8), N1-Zn1-N4 105.42(9), O1-Zn1-N4 96.51(8), N5-Zn1-N4 120.82(8), N1-Zn1-N3 79.53(8), O1-Zn1-N3 179.26(8), N5-Zn1-N3 82.40(8), N4-Zn1-N3 83.53(8), N2-Zn2-O2 107.38(8), N2-Zn2-N8 111.01(9), O2-Zn2-N8 97.46(8), N2-Zn2-N7 116.48(9), O2-Zn2-N7 93.43(8), N8-Zn2-N7 125.07(9), N2-Zn2-N6 79.23(8), O2-Zn2-N6 172.67(8), N8-Zn2-N6 82.73(8), N7-Zn2-N6 80.59(8), O1-C30-O2 127.1(2), O3-C34-N9 131.3(3).

Complex **5** represents an adduct of oxazetidinylacetate with a dinuclear zinc scaffold that is inactive. The carboxylate group of oaa has completely displaced the O_2H_3 bridging unit of the starting complex **4** and is now found in a bidentate bridging mode within the bimetallic pocket, while the β-lactam moiety remains uncoordinated. The zinc ions are five-coordinate (complex **5**: $\tau = 0.86/0.79$) and nested within their respective coordination compartments with a Zn···Zn distance of 4.184 Å. An analogous structure of the $[L^2]^-$ complex was obtained, but is not discussed here due to poor crystal quality.

In contrast to **5**, binding of oaa to the most active complex **3** causes de-coordination of some ligand side arms. In the structurally characterized complex **6**, an oaa substrate

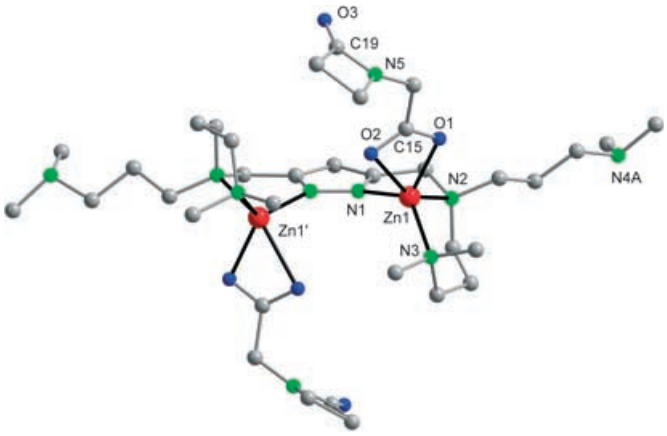

Figure 6. View of the molecular structure of complex **6**. In the interest of clarity, all protons have been omitted. Selected interatomic distances (Å) and angles (°): Zn1–O1 2.006(3), Zn1–O2 2.358(4), Zn1–N1 1.988(4), Zn1–N2 2.156(4), Zn1–N3 2.032(4), Zn1···Zn1′ 4.328(1), N1–N1′ 1.370(7), O1–C15 1.279(6), O2–C15 1.232(6), O3–C19 1.210(6), N5–C19 1.346(6), N1-Zn1-O1 119.8(2), N1-Zn1-N3 125.9(2), O1-Zn1-N3 113.7(2), N1-Zn1-N2 80.7(1), O1-Zn1-N2 96.3(1), N3-Zn1-N2 101.2(2), N1-Zn1-O2 95.8(1), O1-Zn1-O2 59.5(1), N3-Zn1-O2 104.8(2), N2-Zn1-O2 150.0(1), O2-C15-O1 121.1(4), O3-C19-N5 131.7(5). Symmetry transformation used to generate equivalent atoms: (′) $2-x$, $3/2-y$, z.

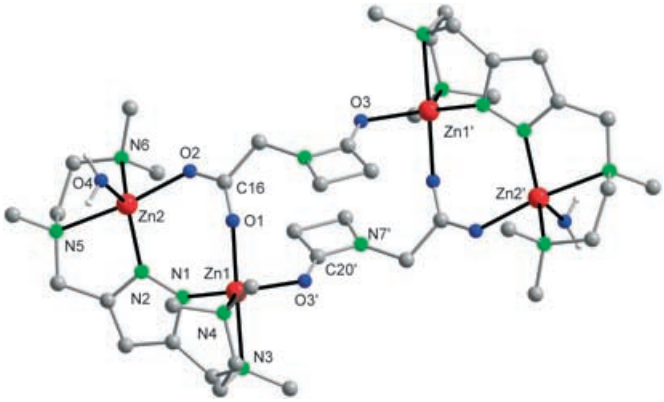

Figure 7. View of the molecular structure of complex **7**. In the interest of clarity, all protons have been omitted. Selected interatomic distances (Å) and angles (°): Zn1–O1 2.093(3), Zn1–O3 2.005(2), Zn1–N1 1.989(3) Zn1–N3 2.232(3), Zn1–N4 2.060(3), Zn2–O2 2.060(2), Zn2–O4 2.031(3), Zn2–N2 1.984(3), Zn2–N5 2.300(3), Zn2–N6 2.121(3), Zn1···Zn2 4.1359(6), O1–C16 1.248(4), O2–C16 1.254(4), O3–C20 1.242(4), N7–C20 1.330(4), N1–N2 1.383(4), N1-Zn1-N3 81.6(1), N2-Zn2-N5 79.3(1), N1-Zn1-N4 115.6(1), N2-Zn2-N6 120.9(1), N1-Zn1-O1 101.7 (1), N2-Zn2-O2 106.7 (1), N1-Zn1-O3′ 129.0(1), N2-Zn2-O4 120.7(1), N3-Zn1-N4 84.8(1), N5-Zn2-N6 82.6(1), N3-Zn1-O1 175.9(1), N5-Zn2-O2 168.8(1), N3-Zn1-O3′ 92.1(1), N5-Zn2-O4 95.3 (1), N4-Zn1-O1 91.4(1), N6-Zn2-O2 86.3(1), N4-Zn1-O3′ 114.1(1), N6-Zn2-O4 116.6(1), O1-Zn1-O3′ 87.8(1), O2-Zn2-O4 89.8(1), O1-C16-O2 126.7(3), O3-C20-N7 129.3(3). Symmetry transformation used to generate equivalent atoms: (′) $3/2-x$, $3/2-y$, $1-z$.

mimic is bound in a semibidentate chelating fashion to each of the zinc ions with one short (2.006(3) Å) and one significantly longer (2.358(4) Å) Zn–O bond, giving rise to a {4+1} environment of the metal ions. The pyrazolate remains as the only bridge between the two zinc ions (d(Zn···Zn) = 4.328(1) Å), while the nitrogen atoms of the dangling side arms are probably involved in hydrogen bonding in a N···H···O(H)···H···N motif with a formal H_3O^+ ion included in the crystal lattice (see Figure S3 in the Supporting Information). However, none of those hydrogen atoms could be located. The solid-state structure of complex **6** suggests that facile de-coordination of individual side arm donors might occur in those systems with longer ligand side arms, due to the lower stability of the six-membered chelate rings.[39,48] This is assumed to also play a major role in the hydrolytic β-lactam cleavage by complexes **1** and **3** in solution, as is corroborated by the NMR experiments described below.

The individual ligand compartments of $[L^2]^-$ and $[L^4]^-$ are reminiscent of tripodal tetradentate ligands tris(pyridylmethyl)amine (tpa) or alkylated derivatives of tris(aminoethyl)-amine (tren), respectively. Dinuclear complexes of ligands HL^2 and HL^4 have previously been shown to favor five-coordination of the metal ions, and hence one may anticipate that all accessible coordination sites in **5** are blocked, that is, additional binding of further weak ligands (such as solvent molecules) is not likely. To investigate whether a higher degree of coordinative unsaturation may induce metal-ion binding of the β-lactam amide, we used the ligand HL^5 which bears fewer chelate side arms. The complex $[Zn_2(L^5)(oaa)(H_2O)]_2(ClO_4)_4$ (**7**) could be obtained in crystalline form, and its molecular structure is shown in Figure 7.

In complex **7**, the carboxylate group of oaa again spans two zinc ions that are preorganized by the pyrazolate-based dinucleating scaffold (d(Zn1···Zn2) = 4.1359(6) Å). Due to the lower denticity of the $[L^5]^-$ donor compartments, additional exogeneous ligands must complete the coordination sphere of zinc. A water molecule is found at Zn2 (and is hydrogen bonded to the two perchlorate counteranions, see Figure S5 in the Supporting Information), while the β-lactam amide oxygen atom of a second $[Zn_2(L^5)(oaa)(H_2O)]^{2+}$ coordinates to Zn1. This gives rise to an overall tetranuclear array of two $\{Zn_2(L^5)\}$ subunits bridged by the two difunctional oaa ligands.

Complex **7** represents the first crystallographically characterized example of β-lactam amide oxygen atom coordination to zinc, and comparison with the structures of complexes **5** and **6** reveals that the amide C–O bond is appreciably lengthened upon coordination (1.242(4) Å in **7** versus 1.218(4) and 1.210(6) Å in **5** and **6**, respectively), while the amide C–N bond is concomitantly shortened (1.330(4) Å in **7** versus 1.354(4) and 1.346(6) Å in **5** and **6**, respectively). This is accompanied by a shift of the β-lactam C=O stretching frequency from 1735 (free oaa) to 1712 cm^{-1} in the IR spectrum of complex **7**, indicating marked polarization of this bond upon coordination. Such polarization is usually proposed to activate the amide moiety for nucleophilic attack. Interestingly, the Zn1–O3 separation involving the β-lactam moiety (d(Zn1–O3) = 2.005(2) Å) is clearly shorter than both $Zn–O_{carboxylate}$ bonds (d(Zn1–O1) = 2.093(3) Å, d(Zn2–O2) = 2.060(2) Å), suggesting considerable strength of the $Zn–O_{amide}$ bond. In methanol, however, the tetranu-

clear assembly largely dissociates, as is evidenced by the intense IR absorption at 1735 cm^{-1} characteristic for "free" β-lactam in solution (a weak shoulder is observed at 1714 cm^{-1}) as well as by the ESI mass spectrum showing a dominant signal for $[Zn_2(L^5)(oaa)_2]^+$. Similarly, $[LZn_2(oaa)_2]^+$ and $[LZn_2(oaa)(ClO_4)]^+$ are the most prominent ions in the ESI mass spectra of solutions containing equimolar amounts of oaa and one of the complexes **1**–**4** in methanol. In the case of **3**/oaa and **4**/oaa, peaks assigned to $[Zn_2(L^3)(oaa)(OH)]^+$, $[Zn_2(L^3)(OH)(ClO_4)]^+$ or $[Zn_2(L^4)(oaa)(OH)]^+$, respectively, are also observed. ^{13}C NMR spectra of **5**·$(ClO_4)_2$, **6**·$(ClO_4)_2$ and **7**·$(ClO_4)_2$ reveal a slight downfield-shift of the carboxylate signal from 175.2 ppm (Na(oaa) in $[D_4]$MeOH) to 176.9 (**5**, $[D_4]$MeOH), 177.6 (**6**, $[D_4]$MeOH), or 177.7 ppm (**7**, $[D_6]$acetone),[49] and at most a minor downfield-shift for the lactamic ^{13}C NMR resonance from 170.4 ppm to 170.4 (**5**), 171.5 (**6**), or 172.5 ppm (**7**). Examination of ^{13}C NMR chemical shifts evidently is of limited value for unambiguously assigning the oaa binding site in solution.

NMR spectroscopy of the reaction mixtures: In the case of dinuclear zinc complexes **1** and **2**, ^1H NMR spectroscopic inspection of the pyridyl protons proved informative to reveal details of substrate binding during the initial stages of penicillin hydrolysis. Figure 8 shows ^1H NMR spectra of the free ligand HL^1, of the dinuclear zinc complex **1**, and of an equimolar mixture of complex **1** and penicillin. The binding of zinc by HL^1 to give complex **1** has a major impact on the chemical shift of the pyridyl signals, which are strongly shifted to lower field. The effect is most pronounced for the hydrogen atoms in the *ortho*- and *para*-positions with respect to the coordinating pyridyl nitrogen atoms.

After mixing equimolar amounts of complex **1** and penicillin G (Figure 8, bottom), a high-field shift of all pyridyl signals relative to that observed for complex **1** and a distinct signal broadening is observed, most evidently for the *o*-H (shifting from 9.1 to 8.8/8.5 ppm) and for the *p*-H (from 8.1 to 8.0/7.6 ppm). Since chemical shifts for the **1**/penicillin G mixture are between those for the free ligand HL^1 and the Zn-bound pyridyl groups in complex **1**, dynamic processes may be assumed in which one or more side-arm donors dissociate from the metal ions upon binding of the substrate. Detachment of some N-donor ligand side arms has previously been confirmed structurally in several complexes of HL^3 (including **6**) and may be explained by the much lower stability of the six-membered chelate rings in **1** and **3** compared to the five-membered rings in **2** and **4**. A favorable consequence of such partial N-donor dissociation is the accessibility of additional binding sites at the two zinc ions after coordination of the penicillin G carboxylate group within the bimetallic pocket. These binding sites are then available, for example, for the activation of water and generation of a nucleophilic Zn-bound hydroxide. In line with these considerations complexes **1** and **3** are the most active, and a gradual decrease of the characteristic lactam signals due to hydrolytic cleavage of the β-lactam ring was observed in the above ^1H NMR experiment for **1**/penicillin G. In contrast to **1**, but in accordance with the higher stability of five-ring chelates relative to the six-ring chelates, complex **2** shows only minor signal broadening and no significant shift of the pyridyl signals upon mixing with penicillin G (see Figure S6 in the Supporting Information). Dissociation of ligand side arms is thus unlikely in this system, though some dynamic processes cannot be fully excluded. Closer inspection of the pyridyl region for the mixture **2**/penicillin G shows several groups of minor peaks around the main signals for **2**. These minor peaks can be explained by binding of the chiral penicillin to the dinuclear zinc scaffold, causing the four pyridine rings to become inequivalent and to give separate signals in the adduct. Though binding of penicillin to **2** evidently occurs, no significant hydrolysis is observed over time. One may conclude that in the substrate-bound complex **2**/penicillin either the substrate is not activated for hydrolysis, or the bimetallic pocket and all coordination sites are blocked, similar to the situation with complex **5**, thus preventing nucleophilic activation at the metal ions. Lower stability of the six-membered chelate rings in **1** and **3** is advantageous in the present systems, since this allows for the binding of the substrate within the bimetallic pocket (presumably through the bridging carboxylate moiety) and simultaneously provides accessible sites for nucleophile activation and/or for binding and polarisation of the β-lactam amide oxygen atom. The molecular structure of complex **7** bearing a ligand scaffold with fewer donor sites corroborates these assumptions.

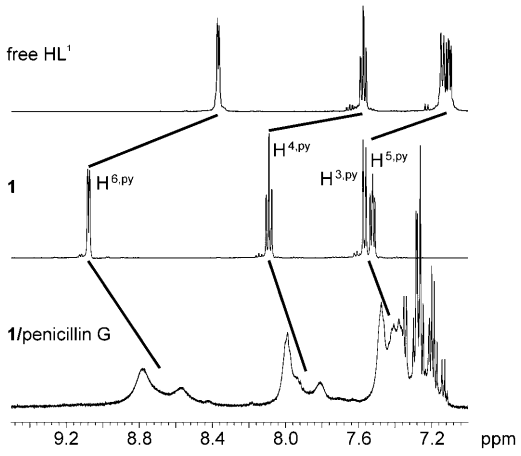

Figure 8. Aromatic region from the ^1H NMR spectra of HL^1 (top), complex **1** (middle), and of an equimolar mixture of **1** and penicillin G (bottom) (500.13 MHz, 300 K, $[D_6]$acetone/D_2O 8:1).

Conclusion

Structure–activity correlations have been deduced for a set of dinuclear zinc(II) complexes that mimick certain features of a natural class of enzymes, dinuclear zinc metallo-β-lactamases. Drastic differences in activity for the hydrolytic cleavage of penicillin G by the various complexes are ascri-

bed to a lack of accessible binding sites after incorporation of the substrate within the bimetallic pockets of complexes **2** and **4**. On the other hand, lower stability of the six-membered chelate rings in **1** and **3** allows for partial detachment of ligand side arms and hence for open sites to be available for nucleophile activation and/or for binding and polarisation of the β-lactam amide oxygen atom. This interpretation is in line with structural findings for adducts between several pyrazolate-based dinuclear zinc scaffolds and the small substrate analogue oxazetidinylacetate (oaa), **5**–**7**. While ligands $[L^4]^-$ (in **5**) and $[L^5]^-$ (in **7**) differ by the number of donor sites, in both **5** and **7** the carboxylate group of oaa is nested within the bimetallic pocket. However, additional binding of water and of the β-lactam amide oxygen atom is only possible in complex **7**, in which open sites are available. The solid-state structure of complex **6** as well as NMR evidence for complex **1** support the idea that the longer side arms in **1** and **3** are hemilabile and can easily detach from the metal ions to liberate accessible coordination sites, which apparently is a prerequisite for β-lactamase activity.

The molecular structures of complexes **5**–**7** provide clear structural confirmation that for β-lactam antibiotics (or related β-lactam derivatives) binding of zinc to the carboxylate group is favored over binding to the β-lactam amide group. However, coordination of the β-lactam amide oxygen atom may still be induced under suitable circumstances (as observed in **7**) or by proper orientation of the substrate within the binding pocket, and this leads to significant changes of the internal geometry of the β-lactam moiety which are likely to facilitate subsequent hydrolytic ring cleavage. It is plausible that electrostatics contribute considerably to the preferential binding of an anionic carboxylate to highly charged dinuclear zinc scaffolds $\{Zn_2(L)\}^{3+}$ (such as in **1**–**4**), but a lower positive charge of the dinuclear zinc array or involvement of the carboxylate in interactions with positively charged protein residues or in strong hydrogen bonding within the enzyme active site may well alter the binding preference in favor of the neutral β-lactam amide moiety.

Experimental Section

General procedures and methods: Compounds **1**, **2**, **3**, and **4** were prepared as reported.[36,37] *N*-benzylazetidinone and sodium oxazetidinylacetate (Na(oaa)) were synthesized according to published procedures;[50,51] analytical data for Na(oaa): ^{1}H NMR (500 MHz, 300 K, [D$_3$]MeOD): $\delta =$ 3.70 (s, 2H; CH_2COO), 3.34 (t, $^3J_{H,H} = 4.0$ Hz, 2H; NCH_2CH$_2$CO), 2.88 ppm (t, $^3J_{H,H} = 4.0$ Hz, 2H; NCH$_2$CH_2CO); ^{13}C NMR (125 MHz, 300 K, [D$_3$]MeOD): $\delta = 175.2$ (*C*OO), 170.4 (*C*(O)N), 46.7 (*C*H$_2$COO), 40.9 (N*C*H$_2$CH$_2$CO), 37.3 ppm (NCH$_2$*C*H$_2$CO); IR (KBr): $\tilde{\nu} = 1747$ (s, C(O)N), 1723 (s, C(O)N), 1618 (s, COO), 1595 cm^{-1} (s, COO); IR (in MeOH): $\tilde{\nu} = 1735$ (s, C(O)N), 1612 cm^{-1} (s, COO). Solvents were dried according to established procedures; penicillin G sodium salt and cephalothin were purchased from Sigma; all other chemicals were purchased from commercial sources and used as-received. Microanalyses were performed by the Analytical Laboratory of the Inorganic Chemistry Institute of the University of Göttingen (Germany). IR spectra were obtained on a Digilab Excalibur spectrometer and recorded either as KBr pellets or in solution using an Axiom Analytical DPR-210 dipper system. ESI-MS spectra were obtained by using a Finnigan MAT LCQ and FAB-MS spectra with a Finnigan MAT 8400. NMR spectra were obtained with a Bruker Avance 500 and were measured at 300 K. The solvent signal was taken as the chemical shift reference ([D$_6$]acetone $\delta_H = 2.04$ ppm, $\delta_C =$ 29.8 ppm; [D$_6$]DMSO $\delta_H = 2.49$ ppm, $\delta_C = 39.7$ ppm).

Synthesis of $[Zn_2(L^4)(oaa)](ClO_4)_2$ (5·(ClO$_4$)$_2$): A solution containing the ligand HL^4 (174 mg, 0.33 mmol) in MeOH (75 mL) was treated with one equivalent of KO*t*Bu (37.3 mg, 0.33 mmol), two equivalents of Zn(ClO$_4$)$_2$·6H$_2$O (248 mg, 0.67 mmol), and one equivalent of Na(oaa) (50.3 mg, 0.33 mmol); the mixture was stirred at room temperature for 4 h. All volatile material was then evaporated under reduced pressure, the residue was taken up in acetone (50 mL) and filtered, and the solution was layered with light petroleum to gradually yield colorless crystals (185 mg, 57%) of the product **5**·(ClO$_4$)$_2$. ^{1}H NMR (500 MHz, 300 K, [D$_3$]MeOD): $\delta = 6.10$ (s, 1H; C$H^{pz,4}$), 4.12 (s, 2H; CH_2COO), 4.04 (s, 4H; pz-CH_2), 3.44 (t, $^3J_{H,H} = 4$ Hz, 2H; CH_2^{oaa}), 3.25 (brs, 4H; CH_2), 3.08–3.15 (m, 4H; CH_2), 2.96 (t, $^3J_{H,H} = 4$ Hz, 2H; CH_2^{oaa}), 2.72–2.93 (m, 20H; CH_2), 2.45 (brs, 4H; CH_2) 1.28 (brs, 12H; CH_3), 0.96 ppm (brs, 12H; CH_3); ^{13}C NMR (125 MHz, 300 K, [D$_3$]MeOD): $\delta = 176.9$, 170.41, 155.35, 100.57, 55.04, 53.18, 52.28, 48.12, 42.13, 37.74, 10.32, 8.32 ppm; IR (KBr): $\tilde{\nu} = 2977$ (m), 2952 (m), 2923 (m), 2879 (m), 1744 (s), 1592 (s), 1463 (m), 1427 (m), 1404 (m), 1320 (m), 1142 (m), 1093 (vs), 912 (w), 797 (w), 738 (w), 692 (w), 623 cm^{-1} (s); MS (ESI): *m*/*z*: 876 (100) $[Zn_2(L)(oaa)(ClO_4)]^+$; elemental analysis calcd (%) for $C_{34}H_{67}Cl_2N_9O_{11}Zn_2 \cdot H_2O$ (979.65): C 40.93, H 6.97, N 12.64; found: C 40.66, H 6.66, N 12.35.

Synthesis of $[Zn_2(L^3)(oaa)_2](H_3O)(ClO_4)_2$ (6·(H$_3$O)(ClO$_4$)$_2$): A solution containing the ligand HL^3 (165 mg, 0.35 mmol) in MeOH (75 mL) was treated with one equivalent of KO*t*Bu (39.7 mg, 0.35 mmol), two equivalents of Zn(ClO$_4$)$_2$·6 H$_2$O (263 mg, 0.71 mmol), and one equivalent of oaa (53.4 mg, 0.35 mmol); the mixture was stirred at room temperature for 4 h. All volatile material was then evaporated under reduced pressure, the residue was taken up in acetone (50 mL), the mixture was filtered, and the solution layered with light petroleum to gradually yield colorless crystals (200 mg, 53%) of **6**·(ClO$_4$)$_2$. ^{1}H NMR (500 MHz, 300 K, [D$_3$]MeOD): $\delta = 6.13$ (s, 1H; C$H^{pz,4}$), 4.05, 4.03, 3.88, 3.46 (t, $^3J_{H,H} = 4$ Hz, 2H; CH_2^{oaa}), 3.00 (t, $^3J_{H,H} = 4$ Hz, 2H; CH_2^{oaa}), 2.81, 2.62, 2.47, 1.92 ppm; all ligand-based signals were very broad; ^{13}C NMR (125 MHz, 300 K, [D$_3$]MeOD): $\delta = 177.6$, 171.5, 153.3, 103.4, 61.7, 58.3, 57.6, 53.1, 52.7, 44.5, 41.7, 37.2, 23.2 ppm; IR (KBr): $\tilde{\nu} = 3604$ (m), 3429 (br), 2963 (m), 2926 (m), 2854 (m), 1735 (s), 1722 (s), 1592 (m), 1480 (m), 1465 (m), 1431 (m), 1390 (m), 1306 (w), 1243 (w), 1182 (w), ~1090 (vs), 1013 (w), 969 (w), 842 (w), 802 (w), 715 (w), 623 (s), 498 cm^{-1} (w); MS (ESI): *m*/*z*: 849 (50) $[Zn_2(L)(oaa)_2]^+$, 820 (70) $[Zn_2(L)(oaa)(ClO_4)]^+$, 766 (60), 738 (55) $[Zn_2(L)(oaa)(OH)]^+$, 709 (65), 467 (100) $[H_2L]^+$.

Synthesis of $[Zn_2(L^5)(H_2O)(oaa)]_2(ClO_4)_4$ (7·(ClO$_4$)$_4$): A solution containing the ligand HL^5 (130 mg, 0.44 mmol) in MeOH (75 mL) was treated with one equivalent of KO*t*Bu (49.2 mg, 0.44 mmol), two equivalents of Zn(ClO$_4$)$_2$·6H$_2$O (327 mg, 0.88 mmol), and one equivalent of Na(oaa) (66.3 mg, 0.44 mmol); the mixture was stirred at room temperature for 4 h. All volatile material was then evaporated under reduced pressure, the residue was taken up in acetone (50 mL), the mixture was filtered, and the solution layered with light petroleum to gradually yield colorless crystals (102 mg, 30%) of the product **7**·(ClO$_4$)$_2$. ^{1}H NMR (500 MHz, 300 K, [D$_6$]acetone): two discrete species can be observed in solution, as clearly identified by the C$H^{pz,4}$ signals: $\delta = 6.19$ and 6.14 ppm; ^{13}C NMR (125 MHz, 300 K, [D$_6$]acetone): two sets of ligand-based signals are observed, $\delta = 177.7$, 172.5, 153.0, 152.9, 101.6, 100.6, 69.2, 57.9, 57.5, 55.9, 55.8, 54.8, 54.5, 48.1, 47.8, 46.8, 46.1, 44.83, 44.77, 42.3, 36.4 ppm; IR (KBr): $\tilde{\nu} = 3016$ (w), 2968 (w), 2920 (w), 2826 (w), 1712 (s), 1618 (s), 1523 (w), 1460 (m), 1434 (m), 1412 (m), 1359 (w), 1321 (m), 1247 (m), 1222 (m), 1154 (s), 1107 (s), 1055 (s), 963 (m), 934 (w), 806 (m), 695 (w), 623 (m), 503 cm^{-1} (w); IR (in MeOH): $\tilde{\nu} = 1735$ (m), 1714 (w), 1613 (m), 1429 (s), 1106 (s), 1005 (vs), 877 cm^{-1} (w); MS (ESI in water): *m*/*z*: 679 (100) $[Zn_2(L)(oaa)_2]^+$, 664 (45), 650 (25) $[Zn_2(L)(oaa)(ClO_4)]^+$, 488 (60) $[Zn(L)(oaa)]^+$, 397 (10) $[H_3L^5(ClO_4)]^+$, 297 (25) $[H_2L^5]^+$; MS (ESI in MeOH): *m*/*z*: 679 (100) $[Zn_2(L)(oaa)_2]^+$, 650 (30) $[Zn_2(L)(oaa)(ClO_4)]^+$, 610 (40), 596 (62); elemental analysis calcd (%) for $C_{40}H_{78}Cl_4N_{14}O_{24}Zn_4 \cdot H_2O$ (1560.54): C 30.79, H 5.17, N 12.57; found: C 30.61, H 5.11, N 12.39.

Hydrolysis of penicillin G: IR spectra were recorded on a Digilab Excalibur FTIR spectrometer equipped with an Axiom Analytical DPR-210 dipper system and an MCT detector. In a typical experiment a solution of the β-lactam in 1 mL of the appropriate solvent mixture (water/DMSO 1:9 (v/v), DMSO/MeOH 1:1 (v/v)) was added to a solution containing the complex at room temperature and the measurement was started. The initial concentrations of the reaction mixtures were $[\text{complex}]_0 = 10.7$ mM and $[\text{penicillin}]_0 = 42.8$ mM. For quantitative evaluation the β-lactam signal, recorded in absorption mode, was integrated and converted into concentration values with the help of a calibration curve.

Binding of cephalothin (ceph): ^{13}C NMR spectroscopic experiments at 308 K were carried out for solutions of cephalothin (0.1 M) and complex (0.1 M) in [D$_6$]DMSO. ^{13}C NMR for free cephalothin: $\delta = 170.4$ (*C*(O)O ester), 169.9 (C(O)N amide), 163.8 (COO), 162.8 (C(O)N lactam), 136.9, 135.1, 126.5, 126.1, 124.8, 111.7, 64.5, 58.5, 57.1, 35.7, 25.1, 20.6 ppm. ^{13}C NMR in the presence of **1**·(ClO$_4$)$_2$ (carbonyl region): $\delta = 170.1$ (*C*(O)O ester), 169.9 (C(O)N amide), 166.7 (COO), 164.1 ppm (C(O)N lactam). ^{13}C NMR in the presence of **2**·(ClO$_4$)$_2$ (carbonyl region): $\delta = 171.2$ (*C*(O)O ester), 170.7 (C(O)N amide), 165.8 (COO), 164.2 ppm (C(O)N lactam).

Binding of oxazetidinylacetate (oaa): ESI mass spectra were collected for solutions that were ~0.5 mM in both oaa and the respective dinuclear zinc complex in methanol. Only the most prominent peaks are listed. **1**/oaa: *m*/*z*: 929 (95) $[Zn_2(L^1)(oaa)_2]^+$, 900 (100) $[Zn_2(L^1)(oaa)(ClO_4)]^+$, 846 (45) $[Zn_2(L^1)(oaa)(HCOO)]^+$; **2**/oaa: *m*/*z*: 873 (35) $[Zn_2(L^2)(oaa)_2]^+$, 844 (100) $[Zn_2(L^2)(oaa)(ClO_4)]^+$, 780 (45) $[Zn_2(L^2)(oaa)_2-pyCH_3]^+$, 687 (25) $[Zn_2(L^2)(oaa)_2-2(pyCH_3)]^+$; **3**/oaa: *m*/*z*: 849 (28) $[Zn_2(L^3)(oaa)_2]^+$, 738 (100) $[Zn_2(L^3)(oaa)(OH)]^+$, 709 (50) $[Zn_2(L^3)(OH)(ClO_4)]^+$; **4**/oaa: *m*/*z*: 905 (85) $[Zn_2(L^4)(oaa)_2]^+$, 876 (80) $[Zn_2(L^4)(oaa)(ClO_4)]^+$, 822 (100) $[Zn_2(L^4)(oaa)(HCO_2)]^+$, 794 (45) $[Zn_2(L^4)(oaa)(OH)]^+$.

^{1}H NMR spectroscopy of the reaction mixtures: A solution containing the penicillin G sodium salt (12.4 μmol) in 150 μL [D$_6$]acetone and D$_2$O (30 μL) was added to a solution of the respective complex (12.4 μmol) in [D$_6$]acetone (500 μL) and D$_2$O (50 μL). ^{1}H NMR spectra were recorded periodically.

X-ray crystallography: Data for complexes **5**, **6** and **7** (Table 1) were collected on a Stoe image plate IPDS II-system (graphite-monochromated $Mo_{K\alpha}$ radiation, $\lambda = 0.71073$ Å) at −140 °C. The structures were solved by direct methods with the SHELXS-97 and refined with the SHELXL-97 programs.[52] The non-hydrogen atoms were refined anisotropically, except those in disordered parts. Hydrogen atoms attached to carbon atoms were refined with a fixed isotropic displacement parameter of 0.08 Å^2. The positional and isotropic thermal parameters of the hydrogen atoms attached to O4 in **7**·(ClO$_4$)$_4$·C$_3$H$_6$O were refined without constraints. Four oxygen atoms of two ClO_4^- moieties in **5**·(ClO$_4$)$_2$ are disordered about two positions (occupancy factors: 0.572(11)/0.428(11) and 0.601(11)/0.399(11)) as well as one −NMe$_2$ group (N4, C13, C14) in **6**·(ClO$_4$)$_2$·H$_3$O (occupancy factors: 0.556(14)/0.444(14)). Additionally the two ClO_4^- in **6**·(ClO$_4$)$_2$·H$_3$O are disordered about special positions and the occupancy factors were fixed at 0.5. Face-indexed absorption corrections were performed numerically with the program X-RED.[53] CCDC-256860 (**5**·(ClO$_4$)$_2$), CCDC-256861 (**6**·(ClO$_4$)$_2$·H$_3$O), and CCDC-256862 (**7**·(ClO$_4$)$_4$·C$_3$H$_6$O) contain the supplementary crystallographic data for this paper. These data can be obtained free of charge from The Cambridge Crystallographic Data Centre via www.ccdc.cam.ac.uk/data_request/cif.

Table 1. Crystal data and refinement details for **5**, **6**, and **7**.

	5·(ClO$_4$)$_2$	**6**·(ClO$_4$)$_2$·H$_3$O	**7**·(ClO$_4$)$_4$·C$_3$H$_6$O
formula	$C_{34}H_{67}Cl_2N_9O_{11}Zn_2$	$C_{35}H_{68}Cl_2N_{10}O_{15}Zn_2$	$C_{43}H_{84}Cl_4N_{14}O_{25}Zn_4$
M_r [g mol^{-1}]	979.61	1070.66	1600.52
crystal size [mm]	0.32×0.29×0.23	0.37×0.28×0.25	0.40×0.13×0.12
crystal system	triclinic	orthorhombic	monoclinic
space group	$P\bar{1}$ (No. 2)	*Ibca* (No. 73)	*C*2/*c* (No. 15)
a [Å]	13.2182(7)	13.4390(11)	35.014(2)
b [Å]	13.2816(8)	17.7891(11)	7.9311(4)
c [Å]	14.1531(8)	40.594(3)	25.1307(16)
α [°]	117.683(5)	90	90
β [°]	93.500(4)	90	111.856(5)
γ [°]	91.622(5)	90	90
V [Å^3]	2191.7(2)	9704.7(12)	6477.2(7)
ρ_{calcd} [g cm^{-3}]	1.484	1.467	1.641
Z	2	8	4
F(000)	1032	4504	3312
hkl range	−14–15, ±15, ±16	−14–15, −18–20, −42–47	±40, −8–9, −28–29
θ range [°]	1.55–24.80	2.15–24.74	1.25–24.64
μ [mm^{-1}]	1.281	1.171	1.716
T_{max}/T_{min}	0.7659/0.6323	0.8190/0.6966	0.8449/0.6875
measured reflections	28120	14000	17508
unique reflections (R_{int})	7493 (0.0317)	4124 (0.0729)	5455 (0.0540)
observed reflections [$I > 2\sigma(I)$]	6657	3024	4272
refined parameters/restraints	529/12	331/9	422/0
goodness-of-fit	1.036	1.055	1.036
*R*1 [$I > 2\sigma(I)$]	0.0348	0.0552	0.0371
*wR*2 (all data)	0.0887	0.1307	0.0890
residual electron density [e Å^{-3}]	0.901/−0.971	0.766/−0.536	0.446/−0.396

Acknowledgements

Funding by the Deutsche Forschungsgemeinschaft (project DFG Me1313/5–1) and the Fonds der Chemischen Industrie is gratefully acknowledged.

[1] M. I. Page, *Acc. Chem. Res.* **1984**, *17*, 144–151.
[2] M. I. Page, A. P. Laws, *Chem. Commun.* **1998**, 1609–1617.
[3] D. J. Payne, *J. Med. Microbiol.* **1993**, *39*, 93–99.
[4] J. M. Frère, *Mol. Microbiol.* **1995**, *16*, 385–395.
[5] K. Bush, *Curr. Pharm. Design* **1995**, *5*, 839–845.
[6] K. Bush, G. A. Jacoby, A. E. Medeiros, *Antimicrob. Agents Chemother.* **1995**, *39*, 1211–1233.
[7] I. Massova, S. Mobashery, *Acc. Chem. Res.* **1997**, *30*, 162–168.
[8] A. Matagne, J. Lamotte-Brasseur, J.-M. Frère, *Biochem. J.* **1998**, *330*, 581–598.
[9] K. Bush, *Clin. Infect. Dis.* **1998**, *27*, 48–53.
[10] Z. Wang, W. Fast, A. M. Valentine, S. J. Benkovic, *Curr. Opin. Chem. Biol.* **1999**, *3*, 614–622.
[11] J. A. Cricco, A. J. Vila, *Curr. Pharm. Des.* **1999**, *5*, 915–927.
[12] J. A. Cricco, E. G. Orellano, R. M. Rasia, E. A. Ceccarelli, A. J. Vila, *Coord. Chem. Rev.* **1999**, *190–192*, 519–535.
[13] A. Carfi, S. Pares, E. Duée, M. Galleni, C. Duez, J. M. Frère, O. Dideberg, *EMBO J.* **1995**, *14*, 4914–4921.
[14] N. O. Concha, B. A. Rasmussen, K. Bush, O. Herzberg, *Structure* **1996**, *4*, 823–836.

[15] J. H. Ullah, T. R. Walsh, I. A. Taylor, D. C. Emery, C. S. Verma, S. J. Gamblin, J. Spencer, *J. Mol. Biol.* **1998**, *284*, 125–136.
[16] A. Carfi, E. Duée, M. Galleni, J.-M. Frère, O. Dideberg, *Acta Crystallogr. Sect. D* **1998**, *54*, 313–323.
[17] S. M. Fabiane, M. K. Sohi, T. Wan, D. J. Payne, J. H. Bateson, T. Mitchell, B. J. Sutton, *Biochemistry* **1998**, *37*, 12404–12411.
[18] N. O. Concha, C. A. Janson, P. Rowling, S. Pearson, C. A. Cheever, B. P. Clarke, C. Lewis, M. Galleni, J.-M. Frère, D. J. Payne, J. H. Bateson, S. S. Abdel-Meguid, *Biochemistry* **2000**, *39*, 4288–4298.
[19] N. Diaz, D. Suárez, K. M. Merz, Jr., *J. Am. Chem. Soc.* **2000**, *122*, 4197–4208.
[20] D. Suárez, N. Diaz, K. M. Merz, Jr., *J. Comput. Chem.* **2002**, *23*, 1587–1600.
[21] D. Suárez, E. N. Brothers, K. M. Merz, Jr., *Biochemistry* **2002**, *41*, 6615–6630.
[22] G. S. Baldwin, A. Galdes, A. O. Hill, B. E. Smith, S. G. Waley, E. P. Abraham, *Biochem. J.* **1978**, *175*, 441–447.
[23] R. M. Rasia, A. J. Vila, *Biochemistry* **2002**, *41*, 1853–1860.
[24] Z. Wang, W. Fast, S. J. Benkovic, *Biochemistry* **1999**, *38*, 10013–10023.
[25] M. H. Valladares, M. Kiefer, U. Heinz, R. P. Soto, W. Meyer-Klaucke, H. F. Nolting, M. Zeppezauer, M. Galleni, J.-M. Frère, G. M. Rossolini, G. Amicosante, H.-W. Adolph, *FEBS Lett.* **2000**, *467*, 221–225.
[26] R. M. Rasia, A. J. Vila, *J. Biol. Chem.* **2004**, *279*, 26046–26051.
[27] C. Prosperi-Meys, J. Wouters, M. Galleni, J. Lamotte-Brasseur, *Cell. Mol. Life Sci.* **2001**, *58*, 2136–2143.
[28] G. L. Estiú, R. M. Rasia, J. A. Cricco, A. J. Vila, M. C. Zerner, *Int. J. Quantum Chem.* **2002**, *88*, 118–132.
[29] Z. Wang, W. Fast, S. J. Benkovic, *J. Am. Chem. Soc.* **1998**, *120*, 10788–10789.
[30] N. V. Kaminskaia, B. Spingler, S. J. Lippard, *J. Am. Chem. Soc.* **2001**, *123*, 6555–6563.
[31] M. I. Page, *Acc. Chem. Res.* **1984**, *17*, 144–151.
[32] a) A. A. M. García, P. G. Navarro, P. J. Martínez de las Parras, R. G. Ortiz, I. H. Blázquez, *Recent Res. Dev. Pure Appl. Anal. Chem.* **2002**, *4*, 89–106; b) P. J. Montoya-Pelaez, G. T. T. Gibson, A. A. Neverov, R. S. Brown, *Inorg. Chem.* **2003**, *42*, 8624–8632; c) N. Diaz, T. L. Sordo, D. Suárez, R. Méndez, J. Marin-Vallacorta, *New J. Chem.* **2004**, *28*, 15–25.
[33] N. V. Kaminskaia, C. He, S. J. Lippard, *Inorg. Chem.* **2000**, *39*, 3365–3373.2.
[34] N. V. Kaminskaia, B. Spingler, S. J. Lippard, *J. Am. Chem. Soc.* **2000**, *122*, 6411–6422.
[35] F. Meyer, P. Rutsch, *Chem. Commun.* **1998**, 1037–1038.
[36] B. Bauer-Siebenlist, F. Meyer, E. Farkas, D. Vidovic, J. A. C. Seijo, R. Herbst-Irmer, H. Pritzkow, *Inorg. Chem.* **2004**, *43*, 4189–4202.
[37] B. Bauer-Siebenlist, F. Meyer, E. Farkas, D. Vidovic, S. Dechert, *Chem. Eur. J.* **2005**, 11, 4349–4360.
[38] F. Meyer, K. Heinze, B. Nuber, L. Zsolnai, *J. Chem. Soc. Dalton Trans.* **1998**, 207–213.
[39] J. Ackermann, F. Meyer, E. Kaifer, H. Pritzkow, *Chem. Eur. J.* **2002**, *8*, 247–258.
[40] J. Ackermann, F. Meyer, H. Pritzkow, *Inorg. Chim. Acta* **2004**, *357*, 3703–3711.
[41] The pK_a for the corresponding acid of a pyrazolate-based dinuclear zinc(II) complex featuring triazacyclononane ligand side arms and a bridging hydroxide was also determined as 8.04 (see refs. [36] and[37]).
[42] M. Ruf, K. Weis, H. Vahrenkamp, *J. Am. Chem. Soc.* **1996**, *118*, 9288–9294.
[43] S. Erhardt, E. Jaime, J. Weston, *J. Am. Chem. Soc.* **2005**, *127*, 3654–3655.
[44] Dinuclear zinc complexes of HL^3 are not sufficiently stable in pure water, thus a solvent mixture with rather low water content had to be used. The exact identity of the species in solution remains unclear for **3** and some liberation of Zn^{2+} cannot be fully excluded even in that solvent mixture.
[45] The solid lines for the traces of **1**, **2**, **3**, and Zn^{2+} result from curve fits using the integrated form of the Michaelis–Menten rate law. We are well aware, however, that use of the Michaelis–Menten equation is not justified for kinetic analysis in the present case, given that the substrate concentration does not greatly exceed catalyst concentration. Unfortunately, any comprehensive kinetic analysis was hampered by the small concentration range available under the experimental setup. Solid lines in Figure 3 are primarily meant as a guide for the eye.
[46] a) M. Assos, R. Panossian, M. Guiliano, *Spectrosc. Lett.* **1984**, *17*, 271–278; b) T. Kupka, *Spectrochim. Acta Part A* **1997**, *53*, 2649–2658; c) J. R. Anacona, J. Serrano, *J. Coord. Chem.* **2003**, *56*, 313–320.
[47] Different solvents or solvent mixtures had to be used in the ESI-MS and NMR experiments, since the solubility of penicillin G and of the complexes in pure acetone or methanol was too low for following the β-lactamase reaction by using the infra-red dipper system or for NMR measurements. Hence, DMSO/water (9:1) or acetone/water (8:1), respectively, were used for those experiments. On the other hand, DMSO and acetone proved less suited for ESI-MS measurements, for which methanol was the solvent of choice despite low solubility of the reactants.
[48] F. Meyer, A. Jacobi, B. Nuber, P. Rutsch, L. Zsolnai, *Inorg. Chem.* **1998**, *37*, 1213–1218.
[49] Na(oaa) is not sufficiently soluble in acetone.
[50] W. Wang, E. J. Roskamp, *J. Am. Chem. Soc.* **1993**, *115*, 9417–9420.
[51] K. H. Baggaley, S. W. Elson, N. H. Nicholson, J. T. Sime, *J. Chem. Soc. Perkin Trans. 1* **1990**, 1513–1520.
[52] G. M. Sheldrick, SHELX-97, Programs for Crystal Structure Solution and Refinement, Universität Göttingen (Germany), **1997**.
[53] STOE & CIE GmbH, X-RED, Darmstadt (Germany), **2002**.

Received: December 10, 2004
Revised: April 4, 2005
Published online: July 8, 2005